Journal of Statistical Mechanics: Theory and Experiment
An IOP and SISSA journal

Cooperativity in sandpiles: statistics of bridge geometries

Anita Mehta[1], **G C Barker**[2] **and J M Luck**[3,4]

[1] S N Bose National Centre for Basic Sciences, Block JD, Sector 3, Salt Lake, Calcutta 700098, India
[2] Institute of Food Research, Colney Lane, Norwich NR4 7UA, UK
[3] Service de Physique Théorique[5], CEA Saclay, 91191 Gif-sur-Yvette cedex, France
E-mail: anita@bose.res.in, barker@bbsrc.ac.uk and luck@spht.saclay.cea.fr

Received 15 July 2004
Accepted 19 October 2004
Published 28 October 2004
Online at stacks.iop.org/JSTAT/2004/P10014
doi:10.1088/1742-5468/2004/10/P10014

Abstract. Bridges form dynamically in granular media as a result of spatiotemporal inhomogeneities. We classify bridges as linear and complex, and analyse their geometrical characteristics. In particular, we find that the length distribution of linear bridges is exponential. We then turn to the analysis of the orientational distribution of linear bridges and find that, in three dimensions, they are *vertically diffusive but horizontally superdiffusive*; thus, when they exist, long linear bridges form 'domes'. Our results are in good accord with Monte Carlo simulations of bridge structure; we make predictions for quantities that are experimentally accessible, and suggest that bridges are very closely related to force chains.

Keywords: sandpile models (theory)

[4] Author to whom any correspondence should be addressed.
[5] URA 2306 of CNRS.

 PII: S1742-5468(04)87997-4 1742-5468/04/P10014+15$30.00

Contents

1. Introduction

The surface of a sandpile cloaks within it a vast array of complex structures—networks of grains whose stability is interconnected, surrounded by pores and necks of void space. Bridges—arch-like structures, where mutual stabilization is a principal ingredient—are prime among these, spanning all manner of shapes and sizes through a granular medium. They can be stable for arbitrarily long times, since the Brownian motion that would dissolve them away in a liquid is absent in sandpiles—the grains are simply too large for the ambient temperature to have any effect. As a result, they can affect the ensuing dynamics of the sandpile; a major mechanism of compaction is the gradual collapse of long-lived bridges in weakly vibrated granular media, resulting in the disappearance of the voids that were earlier enclosed [1]. Bridges are also responsible for the 'jamming' [2] that occurs, for example, as grains flow out of a hopper.

The difficulty of even identifying, leave alone analysing, structures as complex as bridges in a three-dimensional assembly should not be underestimated; such an algorithm now exists, and its use has resulted in the identification and classification of a panoply of bridge configurations generated via numerical simulations [3, 4]. However, even given the presence of such data, it is a far from obvious task to cast it in theoretical terms. In the following, we present a theory for the formation of bridges, which, among other things, is able to explain at least some of the salient features of our numerical data.

We first define a bridge. Consider a stable packing of hard spheres under gravity, in three dimensions. Each particle typically rests on three others, which stabilize it, in the sense that downward motion is impeded. *A bridge is a configuration of particles in which the three-point stability conditions of two or more particles are linked; that is, two or more particles are mutually stabilized.* They are thus structures which cannot be formed by the *sequential* placement of individual particles; they are, however, frequently formed by natural processes such as shaking and pouring, where cooperative effects arise naturally. In a typical packing, up to 70% of particles are involved in bridge configurations. The detailed history of a stabilization process identifies a unique set of bridges, since the stabilizing triplet for each sphere is well defined. While it is impossible to determine bridge distributions uniquely from an array of coordinates representing particle positions,

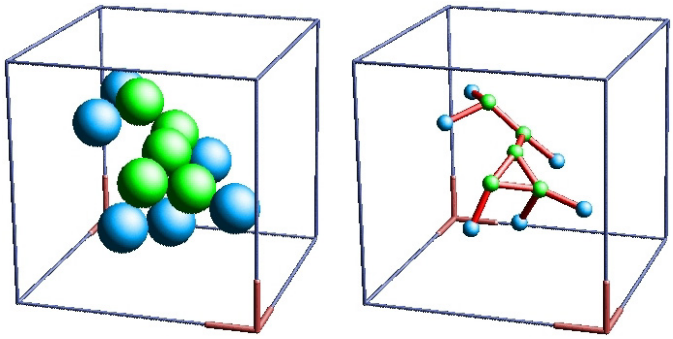

Figure 1. A five particle *complex bridge*, with six base particles (left), and the corresponding contact network (right). Thus $n = 5$ and $n_b = 6 < 5 + 2$.

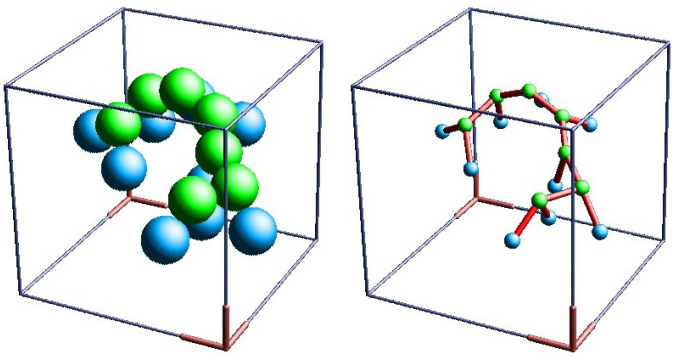

Figure 2. A seven particle *linear bridge* with nine base particles (left), and the corresponding contact network (right). Thus $n = 7$ and $n_b = 9 = 7 + 2$.

we are able via our algorithm to obtain ones that are the most likely to be the result of a given stabilization process [3, 4].

We now distinguish between *linear* and *complex* bridges via a comparison of figures 1 and 2. Figure 1 illustrates a *complex* bridge, i.e., a mutually stabilized cluster of five particles (shown in green), where the stability is provided by six stable base particles (shown in blue). Of course the whole is embedded in a stable network of grains within the sandpile. Also shown is the network of contacts for the particles in the bridge: we see clearly that three of the particles each have two mutual stabilizations. Figure 2 illustrates a seven particle linear bridge with nine base particles. This is an example of a *linear* bridge. The contact network shows that this bridge has a simpler topology than that in figure 1. Here, all of the mutually stabilized particles are in sequence, as in a string. A linear bridge made of n particles therefore always rests on $n_b = n + 2$ base particles, whereas the number n_b of base particles of a complex bridge of size n varies from one bridge to another, and always obeys $n_b < n + 2$, because of the presence of loops in the contact network of complex bridges.

An important point to note is that bridges can only be formed sustainably in the presence of friction; the mutual stabilizations needed would be unstable otherwise! Although we use Monte Carlo simulations (described below) which do not contain friction explicitly, the configurations we generate correspond to those in nature that include

frictional effects. In particular, they generate coordination numbers in a range that is consistent with the presence of friction [1, 5, 6]. Additionally, we have analysed the configurations of molecular dynamics simulations in the limit of high friction[6]; these generate distributions of bridges very similar to our own. Our simulations suggest strong analogies between bridge structure and force distributions in granular media, which have been measured both in experiments [7] and in simulations [8]. This indicates that bridges might be complementary (and experimentally easier) probes of inhomogeneities in these systems.

2. Simulation details

We have examined bridge structures in hard assemblies that are generated by an established, non-sequential, restructuring algorithm [1, 3, 4], whose main modelling ingredients involve *stochastic* grain displacements and *collective* relaxation from them.

This algorithm restructures a stable hard sphere deposit in three distinct stages.

(1) The assembly is dilated in a vertical direction (with free volume being introduced homogeneously throughout the system), and each particle is given a random horizontal displacement; this models the dilation phase of a vibrated granular medium.

(2) The packing is compressed in a uniaxial external field representing gravity, using a low-temperature Monte Carlo process.

(3) The spheres are stabilized using a steepest descent 'drop and roll' dynamics to find a local minimum of the potential energy.

Steps (2) and (3) model the quench phase of the vibration, where particles relax to locally stable positions in the presence of gravity. Crucially, during the third phase, the spheres are able to roll in contact with others; *mutual stabilizations* are thus allowed to arise, mimicking collective effects. The final configuration has a well-defined network of contacts and each sphere is supported, in its locally stable position, through point contacts, by a set of three other spheres uniquely defined. In practice, the final configuration may include a few non-stabilized particles.

The simulation method recalled above builds a sequence of static packings. Each new packing is built from its predecessor by a random process and the sequence achieves a steady state. In the steady state thus obtained, structural descriptors such as the mean packing fraction and the mean coordination number fluctuate about well-defined mean values. The steady-state mean volume fraction Φ is found to lie typically in the range $\Phi \sim 0.55$–0.61. This volume fraction depends on all the parameters of the simulation, and can therefore be adjusted to any desired value in the above range. The mean coordination number is always $Z \approx 4.6 \pm 0.1$. Since for frictional packings the minimal coordination number is $Z = d+1$ [5], this confirms that our three-dimensional configurations correspond to those generated in the presence of friction. In fact, the mean coordination number of molecular dynamics configurations of frictional sphere packings is slightly above 4.5, in the limit of a large friction coefficient [6]. We recall that, in the absence of friction, the

[6] We thank Leo Silbert for letting us use configurations generated from his molecular dynamics simulations, where we have found and analysed the distribution of bridges.

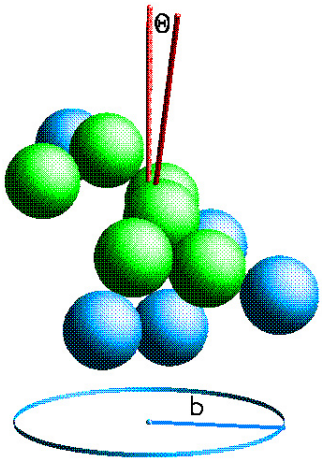

Figure 3. Definition of the angle Θ and the base extension b of a bridge. The main axis makes an angle Θ with the z-axis; the base extension b is the radius of gyration of the base particles about the z-axis.

coordination number is that of an isostatic system, $Z = 2d$ [9], hence $Z = 6$ in the present three-dimensional situation.

To be more specific, simulations were performed in a rectangular cell with lateral periodic boundaries, and a hard disordered base. The simulations, performed serially on a desktop workstation, have a very time-consuming Monte Carlo compression phase with each simulation taking several days' worth of CPU time. This is necessary in order to have simulation results which are reproducible, without appreciable dependence on Monte Carlo parameters or system size. Each of our configurations includes about $N_{\mathrm{tot}} = 2200$ particles. We have examined approximately 100 configurations from the steady states of the reorganization process for the following two values of the packing fraction: $\Phi = 0.56$ and 0.58. Segregation is avoided by choosing monodisperse particles; a rough base prevents ordering. A large number of restructuring cycles is needed to reach the steady state for a given shaking amplitude; about 100 stable configurations (picked every 100 cycles in order to avoid correlation effects) are saved for future analysis. From these configurations, and following specific prescriptions, our algorithm identifies bridges as clusters of mutually stabilized particles [3, 4].

Figure 3 illustrates two characteristic descriptors of bridges used in this work. Along the lines of [4], the *main axis* of a bridge is defined using a triangulation of its base particles. Triangles are constructed by choosing all possible connected triplets of base particles: the vector sum of their normals is defined to be the direction of the main axis of the bridge. The orientation angle Θ is defined as the angle between the main axis and the z-axis. The *base extension* b is defined as the radius of gyration of the base particles about the z-axis (which is thus distinct from the radius of gyration about the main axis of the bridge).

3. Geometrical characteristics. Size and diameter distribution

In the following, we present statistics for both linear and complex bridges; however, it is the former that we analyse in greater detail, both because they are conceptually simpler

and because they are in fact more numerous in our simulations. The latter clearly show that as a linear bridge gets longer, it is increasingly likely to develop branches, whereupon it becomes complex [3, 4].

The formation of either type of bridge in shaken granular media is, of course, a dynamical process; we, however, adopt an ergodic viewpoint [10] here, inspired by the ensemble statistics of bridges generated by our simulations. As in polymer theory [11], we differentiate between linear and complex geometries; in our phenomenology, we regard a linear bridge as a random chain which grows in arc length s by the sequential addition of links to its end, while complex bridges, being branched structures, cannot grow sequentially. This replacement of what is in reality a collective phenomenon by a random walk is somewhat analogous to the 'tube model' of linear polymers [11]: both are simple but efficient effective pictures of very complex problems.

In this spirit, we first address the question of the length distribution of linear bridges. We define the length distribution f_n as the probability that a linear bridge consists of exactly n spheres. We make the simplest and the most natural assumption that a bridge of size n remains linear with some probability $p < 1$ if an $(n+1)$th sphere is added to it, in the above sense. This simple effective picture therefore leads to the exponential distribution

$$f_n = (1-p)p^n. \tag{3.1}$$

This exponential law is a common feature of all models for random 'strings' made of n units, irrespective of the way they are formed. An illuminating example is provided by percolation clusters in one dimension, which are the prototype of random linear objects [12].

The above argument leading to an exponential distribution can alternatively be reformulated as follows, by means of a continuum approach. This will give us the opportunity to introduce a formalism that will be extensively used later. A linear bridge is now viewed as a continuous random curve or 'string', parameterized by the arc length s from one of its endpoints. Within the above picture of a sequential process, we assume that a linear bridge disappears at a constant rate α per unit length, either by changing from linear to complex or by collapsing. The probability $S(s)$ that a given bridge survives at least up to length s thus obeys the rate equation $\dot{S} = -\alpha S$, and therefore falls off exponentially, according to $S(s) = \exp(-\alpha s)$. The probability distribution of the length s of linear bridges therefore reads $f(s) = -\dot{S}(s) = \alpha \exp(-\alpha s)$. This is the continuum analogue of (3.1).

Figure 4 shows a logarithmic plot of numerical data for the length distribution f_n of linear bridges. The data exhibit an exponential fall off of the form (3.1), with $p \approx 0.37$, i.e., $\alpha \approx 0.99$.[7] This exponential decay of the distribution of linear bridges is very accurately observed until $n \approx 12$.

Complex bridges begin to be dominant around $n \approx 8$. For a complex bridge, the number n is now referred to as the 'size' of the bridge. As complex bridges are branched objects, it is natural to expect that their size distribution resembles that of generic randomly branched objects, such as for example lattice animals or critical

[7] Despite its proximity to unity, this value of α has no special significance, as can be seen from the corresponding value of p.

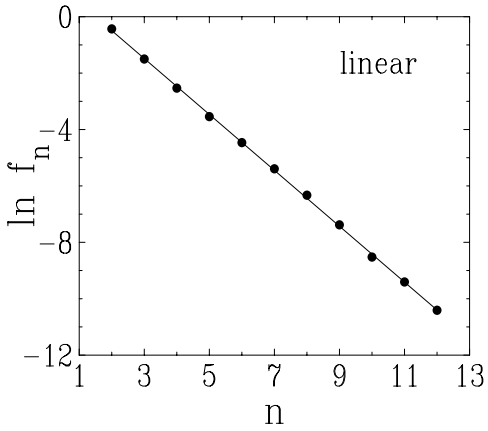

Figure 4. Logarithmic plot of the length distribution f_n of linear bridges, against n, for $\Phi = 0.58$. Full line: least-square fit yielding $p \approx 0.37$, i.e., $\alpha \approx 0.99$.

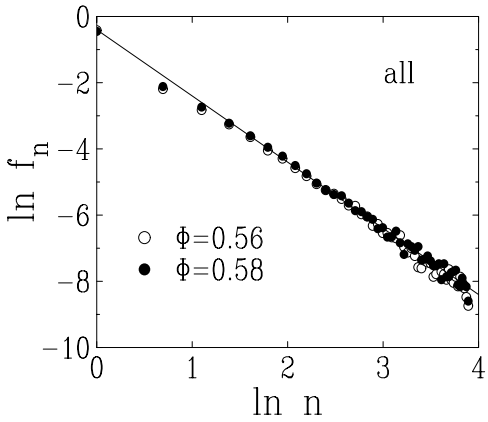

Figure 5. Log–log plot of the size distribution f_n of all bridges, against n, for two volume fractions. This distribution is dominated by complex bridges, since these predominate after $n \sim 8$. Full line: least-square fit yielding $\tau \approx 2.00$.

percolation clusters [12]. These prototypical examples have a power-law fall-off in their size distribution:

$$f_n \sim n^{-\tau}. \tag{3.2}$$

The numerical data shown in figure 5 clearly show that the size distribution of bridges obeys a power-law behaviour of the form (3.2), and thus behave as generic randomly branched objects. The measured value of the exponent τ seems to coincide with the limiting value $\tau = 2$, at and below which the mean size $\langle n \rangle = \sum n f_n$ is divergent.

We now turn to the diameter of linear and complex bridges, which is one of the most important of their geometrical characteristics. The typical diameter R_n of a bridge of size n is such that R_n^2 is the mean squared end-to-end distance over all the bridges of size n. We examine this quantity separately for linear bridges, as well as the ensemble of all bridges. In both cases we expect and find a power-law behaviour

$$R_n \sim n^{\nu}. \tag{3.3}$$

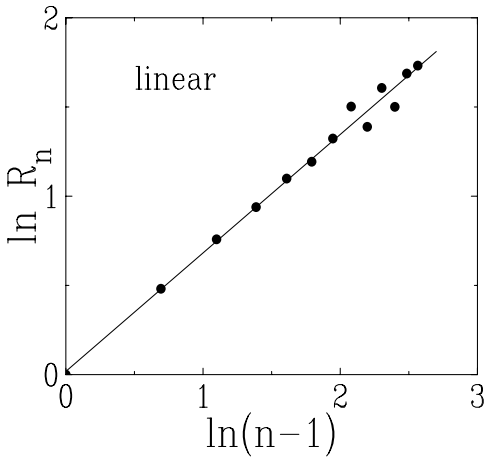

Figure 6. Log–log plot of the typical diameter R_n of linear bridges, against $n-1$, the number of mutually stabilizing bonds, for $\Phi = 0.58$. Full line: least-square fit yielding $\nu_{\rm lin} \approx 0.66$, i.e., $D_{\rm lin} \approx 1.51$.

For linear bridges, $D_{\rm lin} = 1/\nu_{\rm lin}$ can be interpreted as their fractal dimension. The observed value (see figure 6) $\nu_{\rm lin} \approx 0.66$, i.e., $D_{\rm lin} \approx 1.51$, lies between those for a self-avoiding walk in two ($\nu_2 = 3/4$) and three ($\nu_3 \approx 0.59$) dimensions [13]. This seems entirely reasonable, since linear bridges are likely to behave as typical self-avoiding curves. Furthermore, in three dimensions, their effective dimensionality is expected to lie between 2 and 3: they may start off confined to a plane, and then collapse onto each other, due to the effects of vibration.

For complex bridges, we again find a power law of the form (3.3). The geometrical exponent $\nu_{\rm all} \approx 0.74$ (see figure 7) is now naturally compared with the value $\nu \approx 0.875$ of three-dimensional percolation [12]. (Although the figure shows statistics for 'all' bridges, these mostly reflect the behaviour of complex bridges, which dominate beyond about $n \approx 8$.)

Lastly, we plot in figure 8 the probability distribution function of the base extension b, for linear bridges; this is clearly a measure of the spanning, and hence the jamming, potential of a bridge (see figure 3). We also plot in figure 8 distribution functions that are conditional on the bridge size n. This was done to compare our results with those of [14], bearing in mind of course that our results refer to sphere packings in three dimensions whereas theirs refer to disc packings in two. In our case, the conditional distributions are sharply peaked, and only extend over a finite range of b; in theirs the peaks are smaller and the distributions broader. Our results indicate that at least in three dimensions, and up to the lengths of linear bridges probed, bridges of a given length n have a fairly characteristic horizontal extension; we can predict fairly reliably the dimension of the orifice that they might be expected to jam. The results of [14] indicate, on the contrary, that there is a wide range of orifices which would be jammed by disc packings of a given length, in two dimensions. Also, for our three-dimensional bridges, the cumulative distribution has a long tail at large extensions, reflecting chiefly the existence of larger bridges than in the data of [14]. (We note that this long tail is characteristic of three-dimensional experiments on force chains [7, 15] which we will discuss at greater length below.) All of this seems

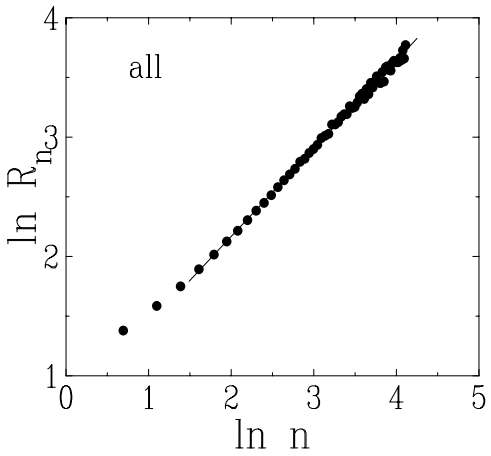

Figure 7. Log–log plot of the typical diameter R_n of all bridges, against size n, for $\Phi = 0.58$. These statistics mainly derive from complex bridges, which dominate beyond about $n \approx 8$. Full line: least-square fit to points with $n > 5$, yielding $\nu_{\text{all}} \approx 0.74$.

entirely reasonable given the more complex topology of three-dimensional space, as well as the greater diversity of possible sphere packings within it.

In the lower part of figure 8 we have plotted the logarithm of the normalized probability distribution of base extensions against the normalized variable $b/\langle b\rangle$, where $\langle b\rangle$ is the mean extension of bridge bases. This figure emphasizes the exponential tail of the distribution function, and also shows that bridges with small base extensions are unfavoured. It is interesting to note that the form of the normalized distribution resembles that found in force distributions of emulsions [16], and that there are also similarities with normal force distributions in MD simulations of particle packings (see e.g. [8, 15]). In our simulations, the sharp drop at the origin with a very tangible peak strongly resembles that obtained in the latter case, in the limit of strong deformations [8]. Realizing that the measured forces [8, 16] propagate through chains of particles, we use this similarity to suggest that our bridges are really just long-lived force chains, which have survived despite strong deformations. We suggest also that with the current availability of three-dimensional visualization techniques such as NMR [17], bridge configurations might be an easily measurable, and effective, tool to probe inhomogeneous force networks in shaken sand.

4. Orientational distribution of linear bridges. Theory and simulation

Linear bridges predominate at small n, which is after all the regime of interest for finite-sized simulations and experiments. The theory we present below focuses on such bridges; the distribution of their orientation is predicted, and then compared with our simulation results.

As before, a linear bridge is modelled as a continuous curve, parameterized by the arc length s from one of its endpoints. We propose the following effective description of the local and global orientation of this curve. For the sake of simplicity, we choose to focus on the most important degree of freedom, which is the tilt with respect to the horizontal;

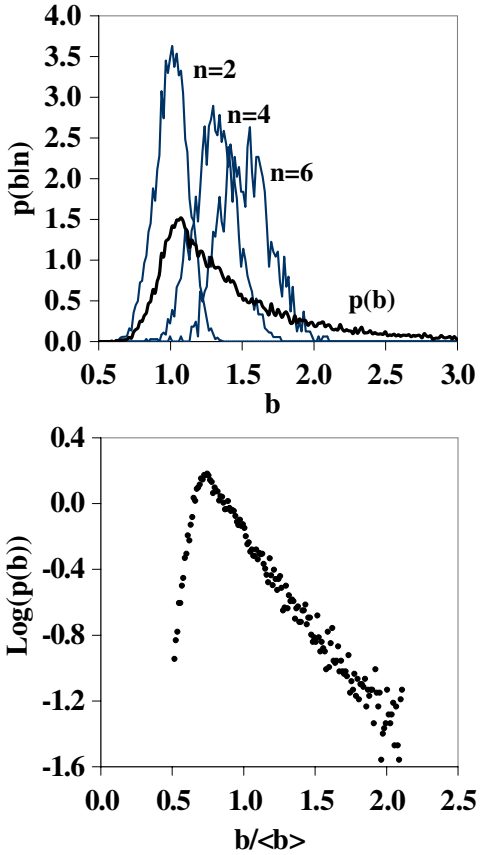

Figure 8. Distribution of base extensions of bridges, for $\Phi = 0.58$. In the top panel, the distributions conditional on the bridge size n, for $n = 2, 4, 6$ are marked in blue, while the cumulative distribution is drawn in black. The bottom panel shows the logarithm of the normalized probability distribution, as a function of the normalized variable $b/\langle b \rangle$.

the azimuthal degree of freedom is therefore neglected. Accordingly, we define the local or 'link' angle $\theta(s)$ between the direction of the tangent to the bridge at point s and the horizontal, and the mean angle made by the bridge from its origin up to point s,

$$\Theta(s) = \frac{1}{s} \int_0^s \theta(u)\, \mathrm{d}u. \tag{4.1}$$

The local angle $\theta(s)$ so defined may be either positive or negative; it can even change sign along the random curve which represents a linear bridge. Of course, the orientation angle Θ measured in our numerical simulations pertains to the three-dimensional realm of real sphere packings. It is there positive by construction, being defined at the end of section 2 as the angle between the main bridge axis and the z-axis.

Our simulations show that the angle $\Theta(s)$ typically becomes smaller and smaller as the length s of the bridge increases. Small linear bridges are almost never flat [3, 4]; as they get longer, assuming that they still stay linear, they get 'weighed down', arching over as at the mouth of a hopper [18]. Thus, in addition to our earlier claim that long linear

bridges are rare, we claim further here that (if and) when they exist, they typically have flat bases, becoming 'domes'.

We use these insights to write down equations to investigate the angular distribution of linear bridges. These couple the evolution of the local angle $\theta(s)$ with local density fluctuations $\phi(s)$ at point s:

$$\dot{\theta} = -a\theta - b\phi^2 + \Delta_1\eta_1(s), \tag{4.2}$$

$$\dot{\phi} = -c\phi + \Delta_2\eta_2(s). \tag{4.3}$$

The effects of vibration on each of θ and ϕ are represented by two independent white noises $\eta_1(s)$, $\eta_2(s)$, such that

$$\langle \eta_i(s)\eta_j(s')\rangle = 2\delta_{ij}\delta(s-s'), \tag{4.4}$$

whereas the parameters $a, \ldots, \Delta_2$ are assumed to be constant.

The phenomenology behind the above equations is the following: the evolution of $\theta(s)$ is caused by the addition to the bridge of single particles to the bridge, along the lines of our effective sequential picture. The motion of particles within their cages gives rise to the fluctuations of local density at a point s; thus ϕ can be regarded as an effective *collective* coordinate, with θ seen as an *independent-particle* coordinate [19].

The individual dynamics are simple: the first terms on the right-hand side of (4.2), (4.3) say that neither θ nor ϕ is allowed to be arbitrarily large. Their coupling via the second term in (4.2) arises as follows: large link angles θ will be increasingly unstable in the presence of density fluctuations ϕ^2 of large magnitude, which would to a first approximation 'weigh the bridge down', i.e., decrease the angle θ locally. Density fluctuations (otherwise known as 'dilatancy') also play a key role in the dynamics of the angle of repose of a sandpile, which are described in a concurrent paper [20]. There, sandpile collapse is described in terms of an activated process, where an effective temperature competes against configurational barriers generated by dilatancy.

Reasoning as above, we therefore anticipate that for low-intensity vibrations and stable bridges, both density fluctuations $\phi(s)$ and link angles $\theta(s)$ will be small. Accordingly, we linearize (4.2), obtaining thus an Ornstein–Uhlenbeck equation [21, 22]

$$\dot{\theta} = -a\theta + \Delta_1\eta_1(s). \tag{4.5}$$

Let us make the additional assumption that the initial angle θ_0, i.e., that observed for very small bridges, is itself Gaussian with variance $\sigma_0^2 = \langle\theta_0^2\rangle$. The angle $\theta(s)$ is then a Gaussian process with zero mean for any value of the length s. Its correlation function can be easily evaluated to be

$$\langle\theta(s)\theta(s')\rangle = \sigma_{\rm eq}^2 \mathrm{e}^{-a|s-s'|} + (\sigma_0^2 - \sigma_{\rm eq}^2)\mathrm{e}^{-a(s+s')}. \tag{4.6}$$

The characteristic length for the decay of orientation correlations is $\xi = 1/a$, and the variance of the link angle reads

$$\langle\theta^2\rangle(s) = \sigma_{\rm eq}^2 + (\sigma_0^2 - \sigma_{\rm eq}^2)\mathrm{e}^{-2as}, \tag{4.7}$$

where

$$\sigma_{\rm eq}^2 = \frac{\Delta_1^2}{a} \tag{4.8}$$

is the 'equilibrium' value of the variance of the link angle. Thus as the chain gets longer, the variance of the link angle relaxes from σ_0^2 (that for the initial link) to $\sigma_{\rm eq}^2$, in the limit of an infinite bridge.

We predict from the above that the mean angle $\Theta(s)$ will have a Gaussian distribution, for any fixed length s. By inserting (4.6) into (4.1), we derive its variance:

$$\langle\Theta^2\rangle(s) = 2\sigma_{\rm eq}^2 \frac{as - 1 + {\rm e}^{-as}}{a^2 s^2} + (\sigma_0^2 - \sigma_{\rm eq}^2)\frac{(1-{\rm e}^{-as})^2}{a^2 s^2}. \tag{4.9}$$

The asymptotic result

$$\langle\Theta^2\rangle(s) \approx \frac{2\sigma_{\rm eq}^2}{as} \approx \frac{2\Delta_1^2}{a^2 s} \tag{4.10}$$

confirms our earlier statement (see below (4.1)) that a typical long bridge has a base that is almost flat. It can be viewed as consisting of a large number $as = s/\xi \gg 1$ of independent 'blobs'[8], each of length ξ.

The result (4.10) has another interpretation. As $\Theta(s)$ is small with high probability for a very long bridge, its extension in the vertical direction reads approximately

$$Z = z(s) - z(0) \approx s\Theta(s), \tag{4.11}$$

so that $\langle Z^2\rangle \approx s^2\langle\Theta^2\rangle(s) \approx 2(\Delta_1/a)^2\, s$. Going back to the discrete formalism, we have therefore

$$Z_n \sim n^{1/2}. \tag{4.12}$$

The vertical extension of a linear bridge is thus found to grow with the usual random-walk exponent 1/2, whereas its horizontal extension exhibits the non-trivial exponent $\nu_{\rm lin} \approx 0.66$ of figure 6. Thus, *long linear bridges are domelike; they are vertically diffusive but horizontally superdiffusive*. We recall that the two-dimensional arches found in [14] were diffusive in a vertical direction; our present results show that, in three dimensions, the vertical diffusivities of bridge structures remain, and are enriched by a horizontal superdiffusivity. Evidently, jamming in a three-dimensional hopper would be caused by the planar projection of such a *dome*.

We now compare these predictions with data from our simulations. The numerical data shown in figure 9 confirm that the mean angle has, to a good approximation, a Gaussian distribution in this typical situation of bridges of size $n = 4$. We recall that the angle Θ measured in simulations pertains to the three-dimensional world. Hence only the positive half of the Gaussian is used for comparison with results of simulations, and the $\sin\Theta$ three-dimensional Jacobian is divided out. It has also been checked to high accuracy (less than 2% r.m.s. deviation for a bin size $\delta\varphi = 5°$) that the azimuthal angle φ of the main bridge axis has the expected flat distribution. Figure 10 shows the measured size dependence of the variance $\langle\Theta^2\rangle(s)$, for both volume fractions. The numerical data are found to agree well with a common fit to the first (stationary) term of (4.9), with a common value of the parameters $\sigma_{\rm eq}^2 = 0.093$ and $a = 0.55$. The 'transient' effects of the second term of (4.9) are invisible with the present accuracy (see below). This observed agreement therefore provides a first confirmation of the validity of our theory, quite remarkable given that it is entirely independent of the simulations. We conclude that in spite of its simplicity, our theory captures the main features of linear bridges.

[8] This is qualitatively reminiscent of a similar problem in polymers, where the de Gennes picture of 'blob' dynamics in dilute solutions gives way to rigid rod-like behaviour; see e.g. [11].

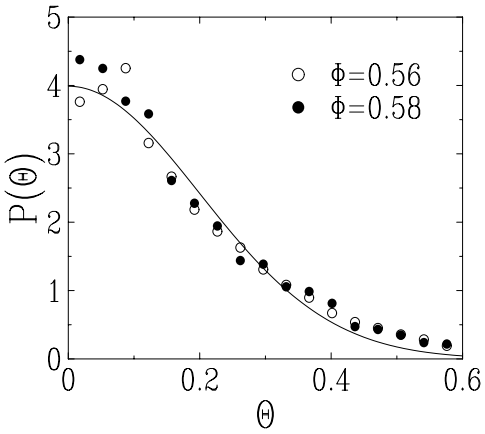

Figure 9. Plot of the normalized distribution of the mean angle Θ (in radians) of linear bridges of size $n = 4$, for both volume fractions. The $\sin\Theta$ Jacobian has been duly divided out, explaining thus the larger statistical errors at small angles. Full curve: common fit to (half) a Gaussian law.

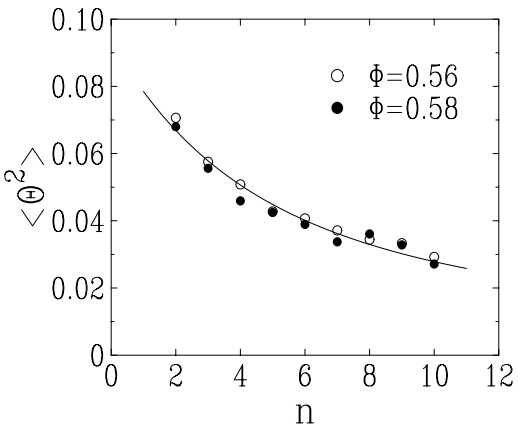

Figure 10. Plot of the variance of the mean angle of a linear bridge, against size n, for both volume fractions. Full curve: common fit to the first (stationary) term of (4.9), yielding $\sigma_{\rm eq}^2 = 0.093$ and $a = 0.55$. The 'transient' effects of the second term of (4.9) are invisible with the present accuracy.

We end this section with the following remarks. First, more subtle effects, including the effects of transients via the second term of (4.9), and the dependence of the parameters $\sigma_{\rm eq}^2$ and a on the packing fraction Φ, are deserving of further investigation. As a preface to our second remark, we recall that in our phenomenological picture linear bridge formation proceeds sequentially, while complex bridges with their branched structures form collectively, in space[9]. We might expect that, with increasing density Φ, branched structures would become more and more common; linear bridge formation, with its 'sequential' progressive attachment of independent blobs would then become more and more rare. Our theory should therefore cease to hold at a limit packing fraction $\Phi_{\rm lim}$, which

[9] We reiterate once again that this effective picture replaces the complexity of the full dynamical picture, where *all* bridges form cooperatively.

is reminiscent of the *single-particle relaxation threshold density* [23], at which the dynamics of granular compaction crosses over from being single-particle (sequential) to collective. Finally, while we have allowed for the local variability of density fluctuations ϕ via (4.3), we have so far not explicitly coupled these to bridge orientations. All of these issues form part of ongoing work, since much more numerical data are needed before a detailed comparison with theory is possible.

5. Discussion

In the above, we have classified bridge structures in granular media as either linear or complex, analysed their structures as obtained in our simulations, and obtained values for some of their more important geometrical exponents. We have also presented a theory for their orientational correlations, which is in reasonably good agreement with our simulations, and, more importantly, makes predictions that can be observed experimentally. Do linear bridges really predominate at short lengths? Do they really cross over to being domelike at large lengths, if they survive? The answers to these and other questions, if obtained experimentally, will not just satisfy what is arguably mere scientific curiosity. Our investigations above suggest that *long-lived bridges are natural indicators of sustained inhomogeneities in granular systems*. Consequently, experimental and theoretical explorations of geometry and dynamics in stable bridge networks will have immediate implications for issues such as hysteresis and cooperative stability, which are some of the most visible manifestations of complexity in granular media.

Acknowledgments

AM warmly thanks SMC-INFM (Research and Development Center for Statistical Mechanics and Complexity, Rome, Italy), and the Service de Physique Théorique, CEA Saclay, where parts of this work were done. GCB acknowledges support from the Biotechnology and Biological Sciences Research Council UK and thanks Luis Pugnaloni for help with the figures. Kirone Mallick is gratefully acknowledged for fruitful discussions.

References

[1] Mehta A and Barker G C, 1991 *Phys. Rev. Lett.* **67** 394
Barker G C and Mehta A, 1992 *Phys. Rev.* A **45** 3435
[2] Jaeger H M, Nagel S R and Behringer R P, 1996 *Rev. Mod. Phys.* **68** 1259
de Gennes P G, 1999 *Rev. Mod. Phys.* **71** S374
[3] Pugnaloni L A, Barker G C and Mehta A, 2001 *Adv. Complex Syst.* **4** 289
[4] Pugnaloni L A and Barker G C, 2004 *Physica* A **337** 428
[5] Edwards S F, 1998 *Physica* **249** 226
[6] Silbert L E *et al*, 2002 *Phys. Rev.* E **65** 031304
[7] Liu C H *et al*, 1995 *Science* **269** 513
Mueth D M, Jaeger H M and Nagel S R, 1998 *Phys. Rev.* E **57** 3164
[8] Erikson J M *et al*, 2002 *Phys. Rev.* E **66** 040301
O'Hern C S *et al*, 2002 *Phys. Rev. Lett.* **88** 075507
[9] Donev A *et al*, 2004 *Science* **303** 990
[10] Edwards S F, 2003 *Challenges in Granular Physics* ed A Mehta and T C Halsey (Singapore: World Scientific)
[11] Doi M and Edwards S F, 1986 *The Theory of Polymer Dynamics* (Oxford: Clarendon)
[12] Stauffer D and Aharony A, 1992 *Introduction to Percolation Theory* 2nd edn (London: Taylor and Francis)

[13] des Cloizeaux J and Jannink G, 1990 *Polymers in Solution. Their Modelling and Structure* (Oxford: Clarendon)
[14] To K, Lai P Y and Pak H K, 2001 *Phys. Rev. Lett.* **86** 71
[15] O'Hern C S *et al*, 2001 *Phys. Rev. Lett.* **86** 111
Landry J W *et al*, 2003 *Phys. Rev.* E **67** 041303
[16] Brujic J *et al*, 2003 *Physica* A **327** 201
[17] See chapters by
Fukushima E, 2003 *Challenges in Granular Physics* ed A Mehta and T C Halsey (Singapore: World Scientific)
Seidler G T *et al*, 2003 *Challenges in Granular Physics* ed A Mehta and T C Halsey (Singapore: World Scientific)
[18] Brown R L and Richards J C, 1966 *Principles of Powder Mechanics* (Oxford: Pergamon)
[19] Mehta A, Needs R J and Dattagupta S, 1992 *J. Stat. Phys.* **68** 1131
Mehta A, Luck J M and Needs R J, 1996 *Phys. Rev.* E **53** 92
Hoyle R B and Mehta A, 1999 *Phys. Rev. Lett.* **83** 5170
[20] Luck J M and Mehta A, 2004 *J. Stat. Mech.: Theor. Exp.* P10015
[21] Uhlenbeck G E and Ornstein L S, 1930 *Phys. Rev.* **36** 823
Wang M C and Uhlenbeck G E, 1945 *Rev. Mod. Phys.* **17** 323
[22] van Kampen N G, 1992 *Stochastic Processes in Physics and Chemistry* (Amsterdam: North-Holland)
[23] Berg J and Mehta A, 2001 *Europhys. Lett.* **56** 784